Molecular Biology of the Cell
Vol. 15, 3485–3496, July 2004

Intracellular Trafficking of Bile Salt Export Pump (ABCB11) in Polarized Hepatic Cells: Constitutive Cycling between the Canalicular Membrane and rab11-positive Endosomes[V]

Yoshiyuki Wakabayashi,*† Jennifer Lippincott-Schwartz,† and Irwin M. Arias*†‡

*Department of Physiology, Tufts University School of Medicine, Boston, Massachusetts 02111; †Cell Biology and Metabolism Branch, National Institute of Child Health and Human Development, National Institutes of Health, Bethesda, Maryland 20892

Submitted October 20, 2003; Revised April 2, 2004; Accepted April 14, 2004
Monitoring Editor: Keith Mostov

The bile salt export pump (BSEP, ABCB11) couples ATP hydrolysis with transport of bile acids into the bile canaliculus of hepatocytes. Its localization in the apical canalicular membrane is physiologically regulated by the demand to secrete biliary components. To gain insight into how such localization is regulated, we studied the intracellular trafficking of BSEP tagged with yellow fluorescent protein (YFP) in polarized WIF-B9 cells. Confocal imaging revealed that BSEP-YFP was localized at the canalicular membrane and in tubulo-vesicular structures either adjacent to the microtubule-organizing center or widely distributed in the cytoplasm. In the latter two locations, BSEP-YFP colocalized with rab11, an endosomal marker. Selective photobleaching experiments revealed that single BSEP-YFP molecules resided in canalicular membranes only transiently before exchanging with intracellular BSEP-YFP pools. Such exchange was inhibited by microtubule and actin inhibitors and was unaffected by brefeldin A, dibutyryl cyclic AMP, taurocholate, or PI 3-kinase inhibitors. Intracellular carriers enriched in BSEP-YFP elongated and dissociated as tubular elements from a globular structure adjacent to the microtubule-organizing center. They displayed oscillatory movement toward either canalicular or basolateral membranes, but only fused with the canalicular membrane. The pathway between canalicular and intracellular membranes that BSEP constitutively cycles within could serve to regulate apical pools of BSEP as well as other apical membrane transporters.

INTRODUCTION

Considerable information is known regarding the biosynthetic pathway followed by plasma membrane proteins in polarized hepatocytes. Some proteins, particularly those having GPI-anchors or single transmembrane domains, are targeted to the basolateral plasma membrane from which they transcytose to the apical domain (Bartles *et al*., 1987; Schell *et al*., 1992). Others, such as several ATP-binding cassette (ABC) transporters, which are critical for biliary composition and secretion, traffic directly from Golgi to the apical (canalicular) plasma membrane (Sai *et al*., 1999; Kipp and Arias, 2000; Slimane *et al*., 2003). What is not known is how these proteins are maintained in the membrane to which they are targeted. Here, we address this question by expressing a yellow fluorescent protein (YFP) construct of the bile acid export pump (BSEP, ABCB11) in WIF-B9 cells and by following its steady-state dynamics through use of photobleaching. Our findings reveal that individual BSEP molecules are not stably associated with the canalicular membrane but undergo rapid cycling between the canalicular membrane and a rab11-containing endocytic compartment. Movement of BSEP between these sites was microtubule dependent, sensitive to actin inhibitors, and unaffected by brefeldin A (BFA), cyclic AMP, taurocholate, or phosphatidylinositol 3-kinase (PI 3-kinase) inhibitors. These results are important for understanding how the polarized state is maintained and potentially regulated.

BSEP represents only one of several ABC transporters in the canalicular membrane. It was chosen for study because it is responsible for ATP-dependent secretion of bile acids (Gerloff *et al*., 1998). Bile acids are detergents that are synthesized in the liver from cholesterol, secreted against a concentration gradient into the bile, and facilitate intestinal emulsification and absorption of dietary lipids. More than 80% of bile acids entering the intestine undergo enterohepatic circulation during which they are absorbed into the portal circulation, returned to the liver and subsequently secreted in bile. Bile acid is the major driving force of bile flow. Inheritable defects in BSEP are manifested by reduced bile acid secretion, intracellular accumulation of bile acids, and hepatocellular damage ("cholestasis", bile secretory failure), which confirms that BSEP is the major, if not exclusive, canalicular bile acid transporter (Strautnieks *et al*., 1998).

The amount of ABC transporters in the canalicular membrane is physiologically regulated by the demand to secrete

Article published online ahead of print. Mol. Biol. Cell 10.1091/mbc.E03–10–0737. Article and publication date are available at www.molbiolcell.org/cgi/doi/10.1091/mbc.E03–10–0737.

[V] Online version of this article contains supporting material. Online version is available at www.molbiolcell.org.

‡ Corresponding author. E-mail address: ariasi@mail.nih.gov.

Abbreviations used: BSEP, bile salt export pump; BFA, brefeldin A.

biliary components in response to the enterohepatic circulation of bile acids and hormone-mediated increase in cyclic AMP (Misra *et al.*, 1998; Kipp *et al.*, 2001). Pulse-chase experiments in rat liver revealed that apical ABC transporters reside in large intracellular pool(s), which were not identified structurally or functionally (Kipp *et al.*, 2001; Schmitt *et al.*, 2001). The present studies were performed to identify putative intracellular BSEP pool(s) and to determine their relationship to BSEP molecules at the canalicular membrane.

MATERIALS AND METHODS

Reagents

The following antibodies were used: mouse monoclonal antibody to rat mannosidase II (53FC3; Berkeley Antibody Company, Richmond, CA); mouse monoclonal antibody to EEA-1, TGN38, rab4, 5, $p150^{Glued}$ (BD Transduction Laboratories, Lexington, KY); rabbit polyclonal antibody to rab11 (Zymed Laboratories, South San Francisco, CA); γ-tubulin (Sigma-Aldrich, St. Louis, MO); polyclonal antiserum to BSEP (Kipp and Arias, 2000); and polyclonal antiserum to cCAM105 (Lin *et al.*, 1991). Cy3-conjugated affinity-purified secondary antibodies, streptavidin, and Cy3-conjugated streptavidin were purchased from Jackson ImmunoResearch Laboratories (West Grove, PA). All other chemicals used were commercial products of highest grade.

Cell Culture

WIF-B9 cells were cultured in a humidified 7% CO_2 incubator at 37°C as described previously (Sai *et al.*, 1999). Cells were grown in modified F12 supplemented with 5% fetal bovine serum, 10 μM hypoxanthine, 40 nM aminopterin, 1.6 μM thymidine, 50 mg/l streptomycin, 200,000 U/l penicillin G, and 0.5 mg/l amphotericin B. For microscopy, cells were plated on 35-mm glass bottom dish (MatTek, Ashland, MA) at 1.4×10^5 cells/dish in complete medium without phenol red.

Construct and Generation of Recombinant Adenovirus

pBK-Bsep cDNA expressing rat BSEP (U69487) (Gerloff *et al.*, 1998) was kindly provided by P.J. Meier (University Hospital, Zurich, Switzerland). The pBSEP-YFP vector was constructed by subcloning the full-length BSEP, which lacks the stop codon, into the *Kpn*I/*Apa*I sites of the multiple cloning site of pEYFP-N1 (BD Biosciences Clontech, Palo Alto, CA). Adenovirus was generated as described previously (He *et al.*, 1998). BSEP-YFP was released as a *Kpn*I/*Not*I fragment that was ligated into pShuttle-CMV. Adenovirus was purified with CsCl (Becker *et al.*, 1994). Purified viral solution was desalted with PD-10 column with Sephadex G25 resin (Amersham Biosciences, Piscataway, NJ), which was equilibrated with 10 mM Tris-HCl (pH 7.4), 137 mM NaCl, 5 mM KCl, 1 mM $MgCl_2$, and was stored at −80°C with 1 mg/ml bovine serum albumin (BSA).

Adenovirus Infection

Three days after plating, WIF-B9 cells were infected with BSEP-YFP adenovirus (10 multiplicity of infection) for 1 h at 37°C. After replacing medium, cells were cultured for 3–4 d and then used for biochemical assays or fluorescence microscopic analysis.

Biotinylation

Canalicular membranes were biotinylated as described with minor modification (Ihrke *et al.*, 1993). Cells grown on glass bottom dishes were washed three times with cold Dulbecco's phosphate-buffered saline ($DPBS^{2+}$) and once with biotinylation buffer (10 mM borate, 137 mM NaCl, 3.8 mM KCl, 0.9 mM $CaCl_2$, 0.52 mM $MgCl_2$, 0.16 mM $MgSO_4$, pH 9.0). Cells were incubated with sNHS-LC biotin (Pierce Chemical, Rockford, IL) (0.5 mg/ml in biotinylation buffer) for 30 min at 4°C. After quenching of nonreacted sNHS-LC biotin, cells were incubated with streptavidin (0.25 mg/ml in $DPBS^{2+}$) for 30 min at 4°C, which binds to basolaterally labeled sNHS-LC biotin. Cells were washed three times with $DPBS^{2+}$, fixed with 4% formaldehyde/$DPBS^{2+}$ at 4°C for 1 min, and permeabilized in methanol for 10 min at 4°C. Cells were then incubated with Cy3-conjugated streptavidin for 30 min at room temperature. After washing with $DPBS^{2+}$, fluorescence images were collected by inverted Nikon Diaphot2 microscope with a 60× oil immersion objective, numerical aperture (NA) 1.40. For subcellular fractionation, WIF-B9 cells grown on 15-cm dish were labeled with sNHS-LC biotin. After washing three times with $DPBS^{2+}$, subcellular fractionation was performed.

Subcellular Fractionation

Fractionation was performed at 4°C. WIF-B9 cells were cultured on 15-cm dishes and infected with BSEP-YFP. After 3–4 d, cells were washed three times with DPBS(−), harvested by scraping with a rubber policeman in DPBS(−), and sedimented for 10 min at 800 × *g*. The cell pellet was resuspended in 4 ml of sucrose buffer (0.25 M sucrose 20 mM Tris-HCl, pH7.4, 1 mM EDTA, protease inhibitors) and homogenized using a Potter-Elvehjem Teflon-glass homogenizer and passaged through a syringe (10 × 27-gauge). The homogenate was centrifuged for 15 min at 800 × *g*. Three milliliters of supernatant were layered on a discontinuous sucrose density gradient consisting of 12 (2.5 ml), 16, 19, 23, 27, 31, 35 (all 5 ml), and 43% (3 ml) sucrose (all wt/wt), 20 mM Tris-HCl, pH 7.4, 1 mM EDTA. The gradient was centrifuged for 60 min at 25,000 rpm in a Beckman Coulter SW 27 rotor and fractionated manually from top to bottom (fraction 1, 3 ml; 2–7, 5 ml each; and 8, remainder). The pelleted material was resuspended with 5 ml of sucrose buffer (fraction 9). Equal aliquots were resolved by SDS-PAGE and transferred onto polyvinylidene difluoride membrane. Protein distributions were determined by immunoblot.

Immunofluorescence

WIF-B9 cells were fixed in 4% formaldehyde/$DPBS^{2+}$ at 4°C for 30 min, permeabilized in 0.3% Tween 20, 1% BSA/$DPBS^{2+}$ for 30 min at room temperature. Primary antibodies in 1% BSA in $DPBS^{2+}$ were added and incubated for 1 h at room temperature. After washing with $DPBS^{2+}$, cells were incubated with anti-mouse or rabbit secondary antibodies.

Confocal and Conventional Fluorescence Microscopy

Cells plated on 35-mm glass bottom dish were maintained in phenol red-free medium and covered with mineral oil. Time-lapse fluorescence videomicroscopy was performed using a Nikon Diaphot 2 inverted microscope (Nikon, Melville, NY) equipped with a 60× oil immersion objective (NA 1.40; Nikon), a custom made heating chamber (37°C), and a 12-bit charge-couple device (CCD) camera ORCA (90 nm $pixel^{-1}$) (Hamamatsu, Bridgewater, NJ), attached to a twofold enlargement tube. Images from the CCD camera were collected directly to RAM with an Apple Power Machintosh G3 equipped with 768 Mbytes of RAM space. Image capturing, processing, and automatic and manual data acquisition were performed using OpenLab software (Improvision, Lexington, MA). Data acquisition times typically ranged from 100–800 ms/image.

Quantitative live cell image analysis was performed using a Leica SP2 (Leica Microsystems, Depew, NY) or Zeiss 510 (Carl Zeiss, Thornwood, NY) inverted confocal microscope with a 63× oil immersion objective, NA 1.32 or 1.40. The confocal pinhole was set fully open. BSEP-YFP molecules were excited at 514 nm and imaged at 520–600 nm. Selective photobleaching was performed with 488 and 514 nm laser line at full power. Live cells were held at 37°C by the ASI 400 air stream incubator (Nevtek, Burnsville, VA). Images were captured at 60- to 120-s intervals. Images of fixed cells were acquired on a Nikon Diaphot 2 inverted microscope or Zeiss 510 inverted confocal microscope.

Image Analysis

Sequence images were exported as single TIFF files. Quantitation of mean fluorescence intensity in selected regions of interest was performed using NIH Image 1.62. Regions of interest were tracked manually. All measurements of fluorescence intensity were corrected for background. The speed of the vesicles was determined by measuring distance moved between two successive frames. Quicktime movies were produced using NIH Image 1.62 or OpenLab 2.0; the contrast of original images was in some cases increased.

RESULTS

WIF-B9 Cells as a Model System for Evaluating BSEP Dynamics In Vivo

The WIF-B9 cell line is a hybrid derived from a human hepatoma and rat fibroblast cell line (Ihrke *et al.*, 1993; Decaens *et al.*, 1996) that expresses many hepatocyte-specific proteins and maintains a polarized plasma membrane that forms a structural and functional bile canaliculus (Decaens *et al.*, 1996; Bravo *et al.*, 1998). WIF-B9 cells do not endogenously express BSEP but do express canalicular ABC transporters MDR1 and MRP2, ecto-enzymes, and cCAM105 (Nies *et al.*, 1998; Sai *et al.*, 1999; Tuma *et al.*, 1999). Adenoviral constructs were required to introduce exogenous genes because WIF-B9 cells were not transfectable by using known nonviral procedures.

WIF-B9 cells were validated previously as a model for studying newly synthesized apical ABC transporter trafficking and bile secretion (Sai *et al.*, 1999). To analyze BSEP localization and trafficking, we infected WIFB9 cells with an adenovirus encoding BSEP-YFP and tested whether this protein targets selectively to the canalicular membrane by using

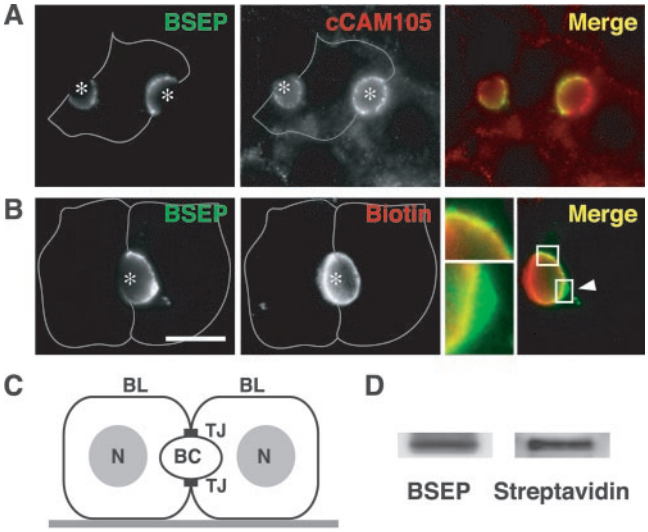

Figure 1. BSEP-YFP targeted to the canalicular membrane in polarized WIF-B9 cells. (A) BSEP-YFP colocalized with cCAM105, a bile canalicular membrane marker. WIF-B9 cells infected with BSEP-YFP adenovirus were fixed and stained with antibody for cCAM105. BSEP and cCAM105 were imaged separately and merged. BSEP-YFP occurs in two hemi-canaliculi of a single cell (asterisk) because adjacent cells were not infected. Antibody to cCAM105 reacted with the entire canalicular membrane and the basolateral membrane (gray line). In the merged image, BSEP-YFP (green) and cCAM105 (red) overlapped at the canalicular membrane (yellow) but not at the basolateral membrane. (B) BSEP-YFP localized in the canalicular membrane and intracellular sites. WIF-B9 cells infected with BSEP-YFP adenovirus were labeled with sNHS-LC biotin at 4°C and incubated with unconjugated streptavidin before fixation. After permeabilization, the biotinylated canalicular membrane was detected with Cy3-conjugated streptavidin. Bar, 10 μm. BSEP-YFP and streptavidin were imaged separately and merged. Gray line denotes basolateral membrane. One cell expressed BSEP-YFP, which visualized half of a bile canaliculus (asterisk). Streptavidin shows canalicular membrane. In the merged image, BSEP-YFP (green) and streptavidin (red) overlapped at the right half of the canalicular membrane (yellow). Several BSEP-YFP intracellular sites were distinct from the canalicular membrane (arrowhead and lower enlarged image). (C) Schematic picture of polarized WIF-B9 cells. BC, bile canaliculus; BL, basolateral membrane; N, nucleli; TJ, tight junction. (D) BSEP-YFP remains at the canalicular membrane. After canalicular membrane biotinylation at 4°C, WIF-B9 cells infected with BSEP-YFP adenovirus were washed, lysed, and immunoprecipitated with antibody for BSEP. Biotinylated BSEP-YFP was detected by SDS-PAGE and Western blotting with HRP-conjugated streptavidin or antibody for BSEP. Immunoprecipitated BSEP-YFP was recognized by HRP-conjugated streptavidin indicating that BSEP-YFP remains at the canalicular membrane.

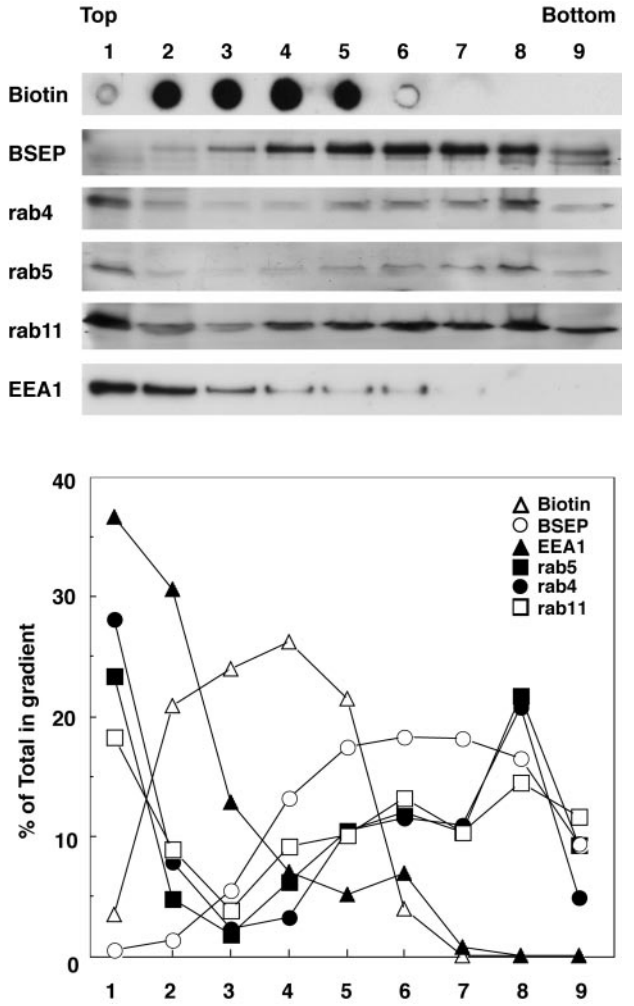

Figure 2. BSEP distributed with endosomal markers in subcellular fractions. WIF-B9 cells infected with BSEP-YFP adenovirus were labeled with sNHS-LC biotin at 4°C, washed, homogenized, and postnuclear supernatants were separated on sucrose step gradients. Aliquots of each fraction were analyzed by SDS-PAGE and Western blotting with antibodies against BSEP, rab4, 5, and 11, and EEA-1 or streptavidin. Fraction 1, homogenization buffer/8% sucrose interphase; fraction 2, 8%/12% interphase; fraction 3, 12%/16% interphase; fraction 4, 16%/19% interphase; fraction 5, 19%/23% interphase; fraction 6, 23%/27% interphase; fraction 7, 27%/31% interphase; fraction 8, 35%/43% interphase; and fraction 9, pelleted material. Bands on gels were quantified by densitometry, and results are expressed as percentage of total amount of each marker in the gradient.

fluorescence microscopy. BSEP-YFP was primarily localized at the bile canalicular membrane domain (Figure 1, A and B), situated between adjacent WIF-B9 cells, which also was labeled with cCAM105, a canalicular adhesion molecule that transcytoses to the apical membrane (Figure 1A). BSEP-YFP was also present in intracellular membranes but was absent from the basolateral plasma membrane (Figure 1, A and B). This distribution resembled that reported for other apical ABC transporter (Sai *et al.*, 1999).

The distribution of BSEP-YFP in canalicular membranes was compared with that of a nonspecific cell surface marker by incubating the cells with a small membrane-impermeable biotin derivative that can access the canalicular membrane through tight junctions (Ihrke *et al.*, 1993). Unconjugated streptavidin, which is too large to pass through tight junctions, was then added, and the cells were incubated at 4°C to prevent endocytosis. Cells were fixed, permeabilized, and incubated with Cy3-conjugated streptavidin. This procedure selectively labeled canalicular membranes (Figure 1B, middle). In addition, BSEP-YFP was localized on internal membranes closely associated with the bile canaliculus that were not accessible to biotin (Figure 1B, arrowhead and enlargement). Additional evidence that BSEP resides within the canalicular membrane was provided when WIF-B9 cells expressing BSEP-YFP were labeled with sNHS-LC biotin, homogenized, immunoprecipitated with BSEP antibodies, and BSEP-YFP was recognized after blotting with by horseradish peroxidase (HRP)-conjugated streptavidin (Figure 1D). These observations indicate that both molecules are present in the canalicular membrane.

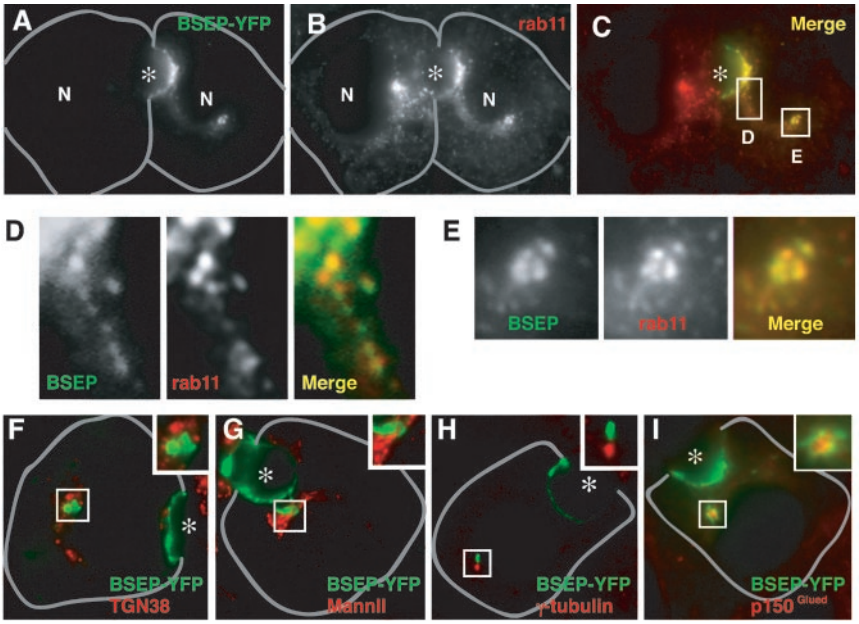

Figure 3. BSEP colocalized with rab11-positive endosomes. After fixation, WIF-B9 cells infected with BSEP-YFP adenovirus were stained with antibody for rab11, TGN38, mannosidase II, γ-tubulin, or p150^{Glued}. Specimens were imaged separately and merged. (A and C) Cell on the right side expressed BSEP-YFP. In addition to the canalicular membrane (asterisk), BSEP-YFP was identified in vesicular structures (D) and perinuclear globular structures (E). (D and E) Enlargements of corresponding areas in C. (B) rab11 distribution in WIF-B9 cells with or without BSEP-YFP expression. (C) A merge of A and B shows that BSEP-YFP (green) localized with rab11 (red) at vesicular tubular structures (D) and perinuclear globular structures (E). (F and G) BSEP-YFP globular structure (green) is separated from Golgi (red), which reacted with antibody for TGN38 (F) and mannosidase II (G). (H and I) BSEP-YFP globular structure (green) is adjacent to the MTOC (red), which stained with antibody for γ-tubulin (H) and p150^{Glued} (I). Bile canaliculus is indicated by asterisk. Gray line shows basolateral membrane.

Biochemical characterization of BSEP-containing membranes was assessed using cell fractionation followed by immunoblotting to confirm the antibody colocalization results. BSEP-YFP adenovirus-infected cells were biotinylated, washed, and homogenized, and postnuclear supernatants were centrifuged in sucrose step gradients. The gradient fractions were subjected to immunoblotting and subsequent densitometry (Figure 2). The plasma membrane was monitored by distribution of biotinylated protein (fractions 2–5). Fraction 1 is the top of the gradient (buffer/8% sucrose interface), which contains soluble proteins. BSEP-YFP sedimented with the plasma membrane (fractions 2–5); the major BSEP-YFP peak was in fractions 5–8. BSEP-YFP was not detected in fraction 1. Rab4, 5, and 11 and EEA1 were primarily detected in fraction 1, which contains protein unbound to membranes. EEA1 distributed in lower density fractions. Rab4, 5, and 11 were detected in all fractions; however, their sedimentation patterns were distinct. Rab4 and 5 were detected equally in fractions 5–7 and peaked in fraction 8. Rab11 was detected equally in fractions 4–9, which is similar to the distribution of BSEP-YFP. These observations reveal that BSEP is present in endosomal components as well as in the plasma membrane.

To identify the intracellular membranes containing BSEP-YFP, WIF-B9 cells expressing the protein were reacted with antibodies to various organelle markers. The distribution of BSEP-YFP overlapped with that detected with antibodies to Rab11 (Figure 3, A–C). Codistribution was observed in tubulo-vesicular intermediates (Figure 3, C and D), membranes adjacent to the bile canaliculus (Figure 3C), and globular perinuclear structures (Figure 3E). These structures contained BSEP-YFP and rab11 and were always proximal to or associated with the microtubule-organizing center (MTOC) as identified with antibodies to γ-tubulin or p150^{Glued} (a dynein component) (Paschal *et al.*, 1993) (Figure 3, H and I) as reported previously for rab11-containing membranes in other cells (Ullrich *et al.*, 1996; Casanova *et al.*, 1999). No colocalization of BSEP-YFP was observed with other organelle markers, including: TGN38 (Figure 3F) and mannosidase II (Figure 3G), which label TGN and Golgi; LAMP 2a, which labels lysosomes, and EEA-1 and rab4, which label early endosomes (our unpublished data).

Distribution of BSEP-YFP in Live WIF-B9 Cells

Quantitation by confocal microscopy of the different pools of BSEP-YFP in live cell preparations revealed that 39.9 ± 17.3% (n = 17) was associated with the canalicular membrane region, 10.4 ± 5.7% with a cytoplasmic globular structure, and the remaining 49.7 ± 17.4% in diffusely distributed tubulo-vesicular structures. Live cells were used because all subsequent dynamic studies were performed in living cells.

BSEP-YFP in the Canalicular Membrane Constitutively Exchanges with BSEP-YFP in Intracellular Compartments

To determine whether BSEP-YFP stably resides at the canalicular membrane or traffics to and from rab11-positive intracellular compartments, we performed selective photobleaching experiments. The canalicular membrane area of BSEP-YFP–expressing cells was selectively photobleached using a confocal system and fluorescence recovery into the bleached region was monitored over time (Figure 4, A and B, and Video 1). Extensive recovery of BSEP-YFP into the photobleached region occurred within 20 min (Figure 4, A and B, and Video 1), indicating that BSEP-YFP at the canalicular membrane undergoes exchange with BSEP-YFP in other compartments. The recovered pool of BSEP-YFP did not result from new protein synthesis because total cellular BSEP-YFP fluorescence levels remained constant for up to 5 h after protein synthesis was blocked by cycloheximide (50 μg/ml), and fluorescence recovery rate is not impaired (our unpublished data). To determine the synthesis rate for BSEP-YFP, the entire cell was photobleached; cellular and canalicular membrane fluorescence did not recover in 2.5 h (Figure 4C).

To test whether the different intracellular pools of BSEP-YFP exchanged with each other in addition to exchanging with the canalicular membrane, BSEP-YFP fluorescence in the globular structure adjacent to the MTOC was selectively photobleached. Fluorescence recovered in 15 min (Figure 5, A and B, and Video 2), indicating that BSEP-YFP molecules do not permanently reside within the globular structure but traffic to other BSEP-containing membranes. Repetitive photobleaching of BSEP-YFP fluorescence at the canalicular membrane resulted in a gradual decrease in BSEP-YFP fluorescence in the globular structure (Figure 5, C and D). This suggests that BSEP-YFP

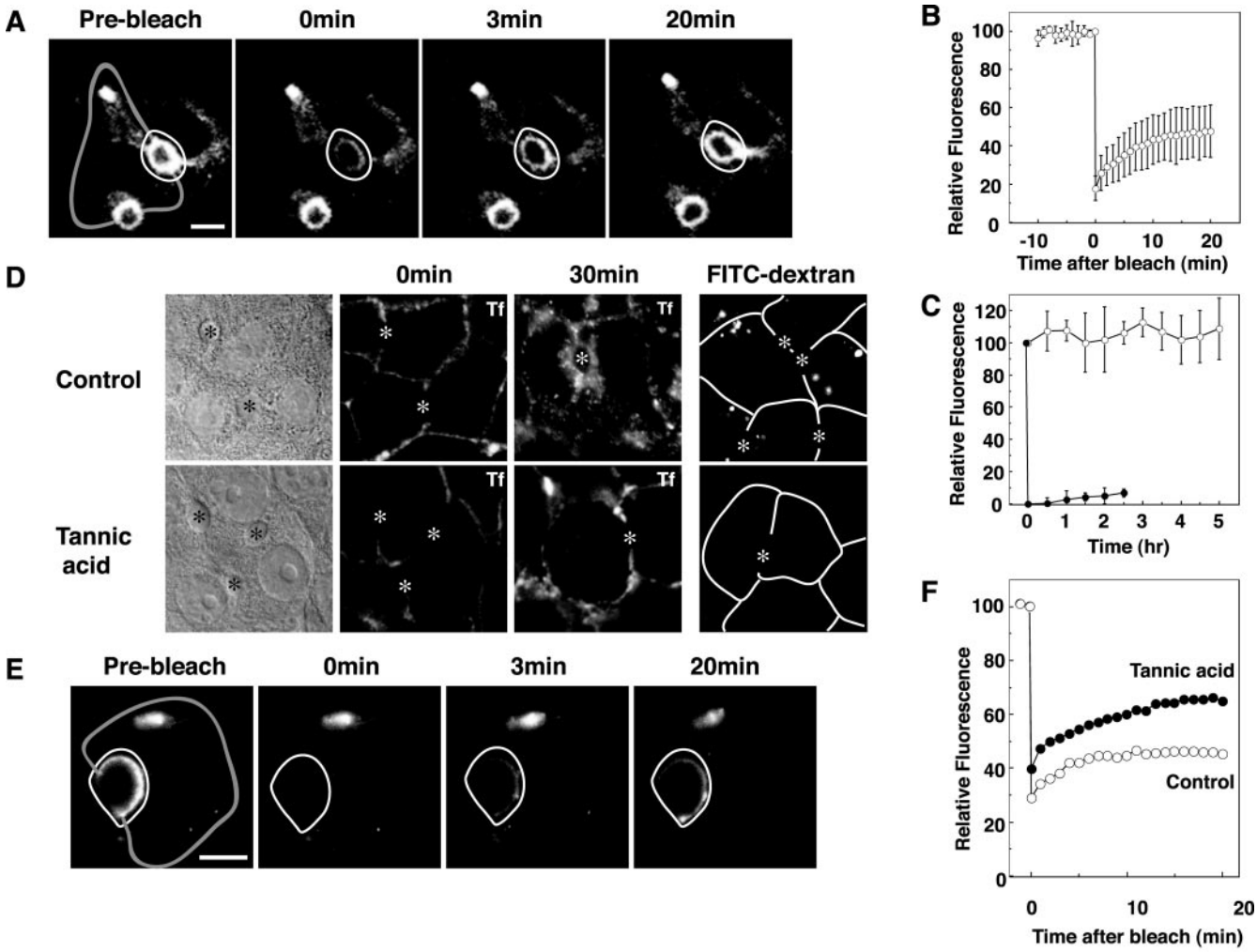

Figure 4. Canalicular BSEP pool constitutively exchanges with other intracellular pools. Also see Videos 1 and 4. WIF-B9 cells infected with BSEP-YFP adenovirus were used for live cell imaging by confocal or conventional fluorescent microscopy at 37°C. (A) Canalicular membrane region BSEP-YFP recovers after photobleach. The area enclosed by a white line was photobleached. Time in the next two panels denotes minutes postbleach. Gray line shows basolateral membrane. (B) Quantitation of BSEP-YFP recovery in the canalicular membrane region after photobleaching (as in A). Mean fluorescence intensity was determined at the times indicated. n = 6 ± SD. (C) Synthesis and degradation of BSEP-YFP. To determine BSEP-YFP synthesis rate, WIF-B9 cells infected with BSEP-YFP adenovirus were photobleached throughout the cell. Fluorescence images were captured at 30-min intervals (solid circles, n = 6 ± SD). To determined BSEP-YFP degradation rate, WIF-B9 cells infected with BSEP-YFP adenovirus were treated with cycloheximide (50 μg/ml). Fluorescence images were captured at 30-min intervals (open circles, n = 6 ± SD). (D) Tannic acid blocked basolateral endocytosis. WIF-B9 cells were incubated with (bottom) or without (top) tannic acid (0.5%) in serum-free medium for 5 min at 37°C. Cells were washed and assayed for uptake of Cy5-conjugated transferrin (Tf) in serum-free medium after 30-min incubation at 0°C (center) or 37°C (right), or uptake of fluorescein isothiocyanate conjugated dextran (mol. wt. 580,000) after 10-min incubation at 37°C. Bile canaliculus is indicated by asterisk. Transferrin and dextran were endocytosed from basolateral membrane in control cells. Tannic acid treatment impaired transferrin and dextran endocytosis from the basolateral membrane. Bile canaliculus is indicated by asterisk. White line shows basolateral membrane. (E) WIF-B9 cells infected with BSEP-YFP adenovirus were incubated with tannic acid (0.5%) in serum-free medium for 5 min at 37°C. The cells were washed and the area enclosed by the white line was photobleached. Time in the second two panels denotes minutes postbleach. Gray line shows basolateral membrane. (F) Quantitation of BSEP-YFP recovery in the canalicular BSEP pool after tannic acid treatment. The canalicular membrane region was photobleached as shown in E. Fluorescence intensity was determined at the times indicated. Open circles denote control values and solid circles are values after tannic acid treatment. (E and F) Tannic acid did not alter BSEP-YFP recovery in the canalicular region.

molecules move from the globular structure to canalicular membranes as part of their normal transport itinerary. Photobleaching of BSEP-YFP fluorescence in the entire cell except the canalicular membrane resulted in gradual recovery of fluorescence in the globular structure and decline in canalicular membrane fluorescence (Figure 5, E and F). When fluorescence in the canalicular membrane and globular structure were simultaneously photobleached, fluorescence in both compartments recovered simultaneously within 30 min (Figure 5, G and H, and Video 3) from fluorescence elsewhere in the cell (including from tubulo-vesicles). Thus, BSEP-YFP molecules rapidly circulate between all BSEP-containing intracellular sites and the canalicular membrane.

We next tested whether perturbation of membrane uptake at the basolateral surface of WIF-B9 cells affects BSEP-YFP cycling between internal and canalicular membranes. This was accomplished by incubating WIF-B9–expressing cells with tannic acid, a plant-derived polyphenol that blocks endo- and exocy-

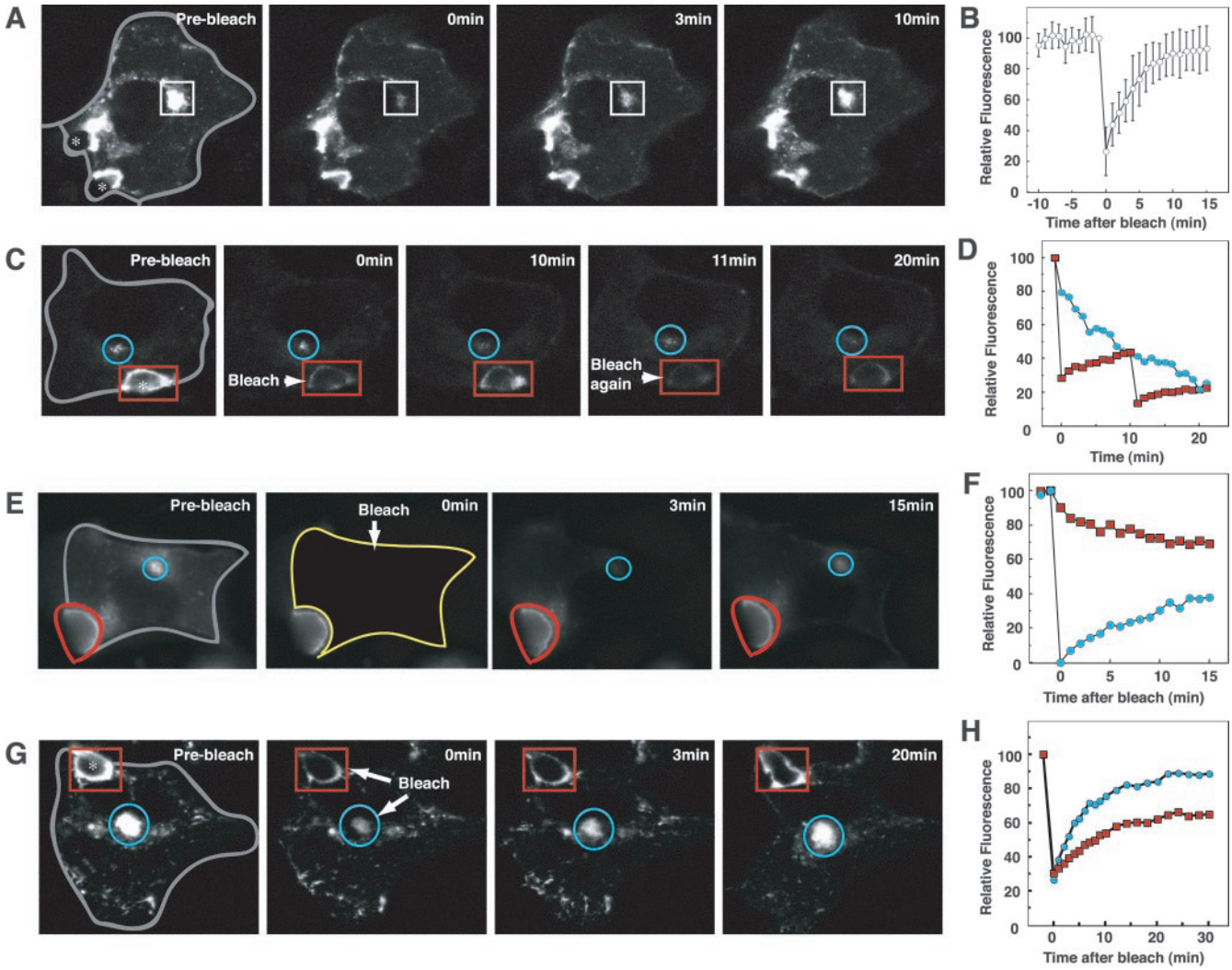

Figure 5. BSEP-YFP constitutively cycles between the canalicular membrane, globular structure and transport carriers. Also see Videos 2 and 3. WIF-B9 cells infected with BSEP-YFP adenovirus were used for live cell imaging by confocal or conventional fluorescence microscopy at 37°C. (A) Globular pool of BSEP-YFP recovered after photobleaching. The area in the box was photobleached. Time in the next two panels denotes minutes postbleach. Gray line shows basolateral membrane. Asterisk shows bile canaliculus. (B) Quantitation of BSEP-YFP recovery in the globular structure pool. The pool was photobleached as shown in A. Mean fluorescence intensity was determined as indicated. n = 6 ± SD. (C) BSEP-YFP loss in the globular pool after photobleaching of the canalicular pool. The canalicular area (red) was photobleached at 0 and again at 10 min. Time in the other panels denotes minutes postbleach. Blue circle indicates the globular pool. Gray line shows basolateral membrane. (D) Quantitation of BSEP-YFP loss in the globular pool. The canalicular area was photobleached at 0 and again at 10 min as shown in C. Blue circles denote globular structure pool, and red squares are canalicular membrane pool values. (E) BSEP-YFP loss in the canalicular pool after photobleaching the entire intracellular BSEP-YFP pool (yellow line). Time in subsequent two panels denotes minutes postbleach. Blue line indicates the globular region and red is the canalicular region. (F) Quantitation of BSEP-YFP fluorescence in the canalicular membrane and globular structure pools as described for E. Blue denotes globular structure pool and red is the canalicular membrane pool. (G) The canalicular membrane domain (red) and globular structure (blue) were photobleached simultaneously. Time in subsequent two panels denotes minutes postbleach. Gray line shows basolateral membrane. (H) Quantitation of BSEP-YFP recovery in the canalicular membrane and globular structure pools as described for G. Blue denotes globular structure pool and red is the canalicular membrane region.

tosis (Newman *et al.*, 1996; Polishchuk *et al.*, 2004). Due to the inability of tannic acid to pass through tight junctions, only basolateral membranes were affected by this treatment. Under these conditions, we observed no uptake of Cy5-conjugated transferrin, a marker of clathrin-mediated endocytosis, or fluorescein isothiocyanate-dextran, a marker for nonclathrin-mediated endocytosis from basolateral membranes (Figure 4D); nevertheless, upon photobleaching BSEP-YFP fluorescence in the canalicular membrane, full recovery of fluorescence from intracellular pools occurred (Figure 4, E and F, and Video 4). These observations indicate that the intracellular pathway followed by BSEP-YFP molecules does not depend on basolateral endocytic traffic.

Characteristics of BSEP-YFP–containing Transport Intermediates

Time-lapse imaging revealed that tubule intermediates were continually dissociating from the globular perinuclear structure, which contains BSEP-YFP (Figure 6, A and B, and Video 5). After detaching, the carriers changed speed and direction (Figure 6D and Video 5) and moved at a maximal rate of 0.85 μm/s to either canalicular or basolateral mem-

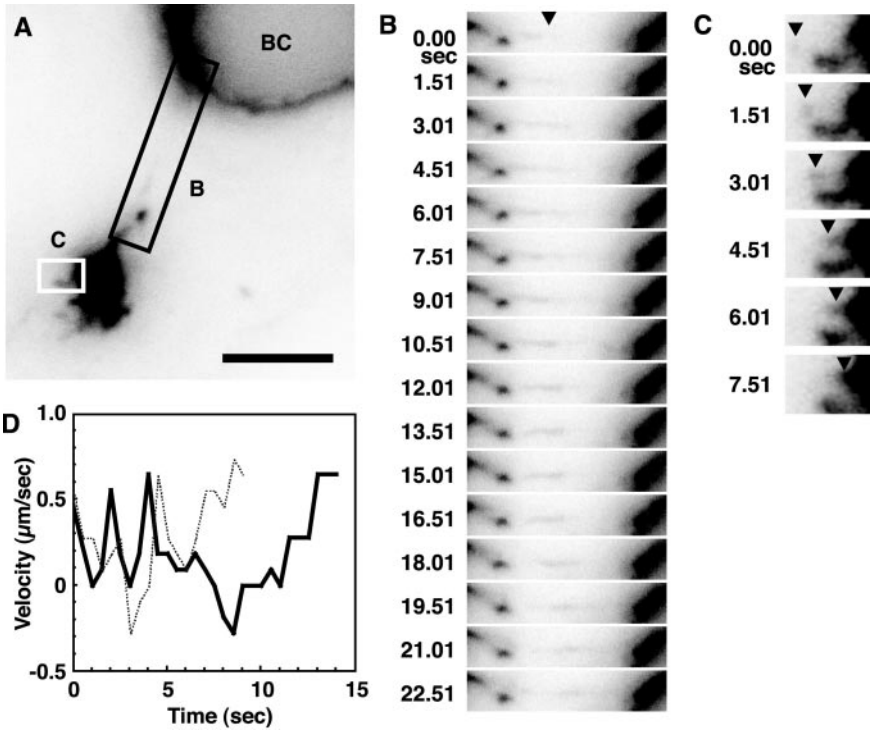

Figure 6. Dynamics of BSEP-YFP transport carrier segregation and fusion in the globular structure and canalicular region. Also see Video 5. (A) WIF-B9 cells infected with BSEP-YFP adenovirus were used for live cell imaging at 37°C with a conventional fluorescence microscope equipped with CCD camera. Bar, 5 μm. The areas in A designated B and C are placed in the corresponding panels. (B) BSEP-YFP transport carriers elongate from the globular structure. Times are relative to the first image in the series. Arrowhead shows BSEP elongation sites. (C) Small transport carriers fuse with globular structure at other sites (arrowhead). Times are relative to the first image in the series. (D) Velocity of two exocytic transport carriers from globular structure. Velocity was measured as the distance between pixel coordinates in consecutive images.

branes (Figure 6B and Video 5). BSEP-YFP–containing transport intermediates that trafficked toward and along the basolateral membrane (Figure 7, A and B, and Video 6) never fused with these membranes. Instead, they returned to the globular structure (Figure 7C and Video 6) with which they fused (Figure 6, A and C, and Video 5). These results indicate that BSEP-YFP–containing carriers traffic throughout the cell but specifically fuse with the canalicular plasma membrane.

Properties of BSEP-YFP Intracellular Trafficking

The role of microtubules in BSEP-YFP trafficking was tested by examining the effects of microtubular disruption by nocodazole treatment. The amount and distribution of BSEP-YFP at the canalicular membrane and globular structure were unchanged in nocodazole-treated cells (Figure 8A); however, as detected by immunofluorescence, rab11 was substantially reduced from the BSEP globular structure (our unpublished data). Furthermore, no restoration of fluorescence was observed after selective photobleaching of the globular structure (Figure 8, A and B). When the canalicular pool of BSEP-YFP was photobleached, fluorescence recovery was inhibited (Figure 8, C and D). After photobleaching of the noncanalicular region of WIF-B9 cells, canalicular fluorescence was significantly retained compared with controls (Figure 8, E and F). In addition, no movement of BSEP-YFP–containing transport intermediates was observed in nocodazole-treated cells. Thus, microtubules play an essential role in BSEP-YFP trafficking.

Actin depolymerizing reagents, such as cytochalasin D and latrunculin A and B, disrupted recycling of the transferrin receptor in polarized epithelial cells (Durrbach *et al.*, 2000), and cytochalasin D inhibited apical endocytosis of receptors in polarized epithelial cells (Gottlieb *et al.*, 1993). To determine the role of actin in BSEP trafficking, we treated cells with cytochalasin D and latrunculin A (Rosin-Arbesfeld *et al.*, 2001). After incubation of WIF-B9 cells in cytochalasin D, canalicular fluorescence increased by 30% (Figure 9A). As shown in Figure 9B, after photobleaching the bile canalicular region in cytochalasin D-treated cells, canalicular fluorescence was restored at the same rate as in control cells. Similar results were observed after treatment of cells with latrunculin A (5 μM) (our unpublished data). After photobleaching of the noncanalicular region of WIF-B9 cells, canalicular fluorescence was significantly retained as compared with controls (Figure 9, D and E). These observations suggest that actin polymerization is required for endocytosis of BSEP from the canalicular membrane.

A fungal metabolite, BFA, inhibits a guanine nucleotide exchange factor for the ADP-ribosylation factor family of small GTPases and leads to redistribution of coat proteins from membranes to the cytoplasm (Chardin and McCormick, 1999). In Madin-Darby canine kidney (MDCK) cells, BFA treatment increased apical endocytosis (Prydz *et al.*, 1992) and inhibited basolateral-to-apical transcytosis (Hunziker *et al.*, 1991). To determine whether BFA affects BSEP-YFP apical cycling, cells were incubated with BFA. Although Golgi structure was disrupted (our unpublished data), the globular structure containing BSEP-YFP was unaffected (Figure 10A). Moreover, no change in the recovery rate of BSEP-YFP fluorescence into photobleached canalicular membrane was observed in BFA-treated cells (Figure 10D). Thus, BSEP trafficking is unaffected by BFA treatment.

PI 3-kinase lipid products affect several membrane trafficking pathways. In WIF-B9 cells, concentrations of wortmannin or LY294002 that selectively inhibit PI 3-kinase activity induced endocytosis of some, but not all, apical membrane proteins and enhance traffic to prelysosomal vacuoles (Tuma *et al.*, 1999; Tuma *et al.*, 2001). We investigated whether PI 3-kinase regulates constitutive BSEP-YFP apical cycling. After incubation of WIF-B9 cells with wortmannin or LY294002, large vacuolar structures occurred (Figure 10B) as demonstrated previously (Tuma *et al.*, 1999), but BSEP-YFP did not accumulate in these structures (Figure

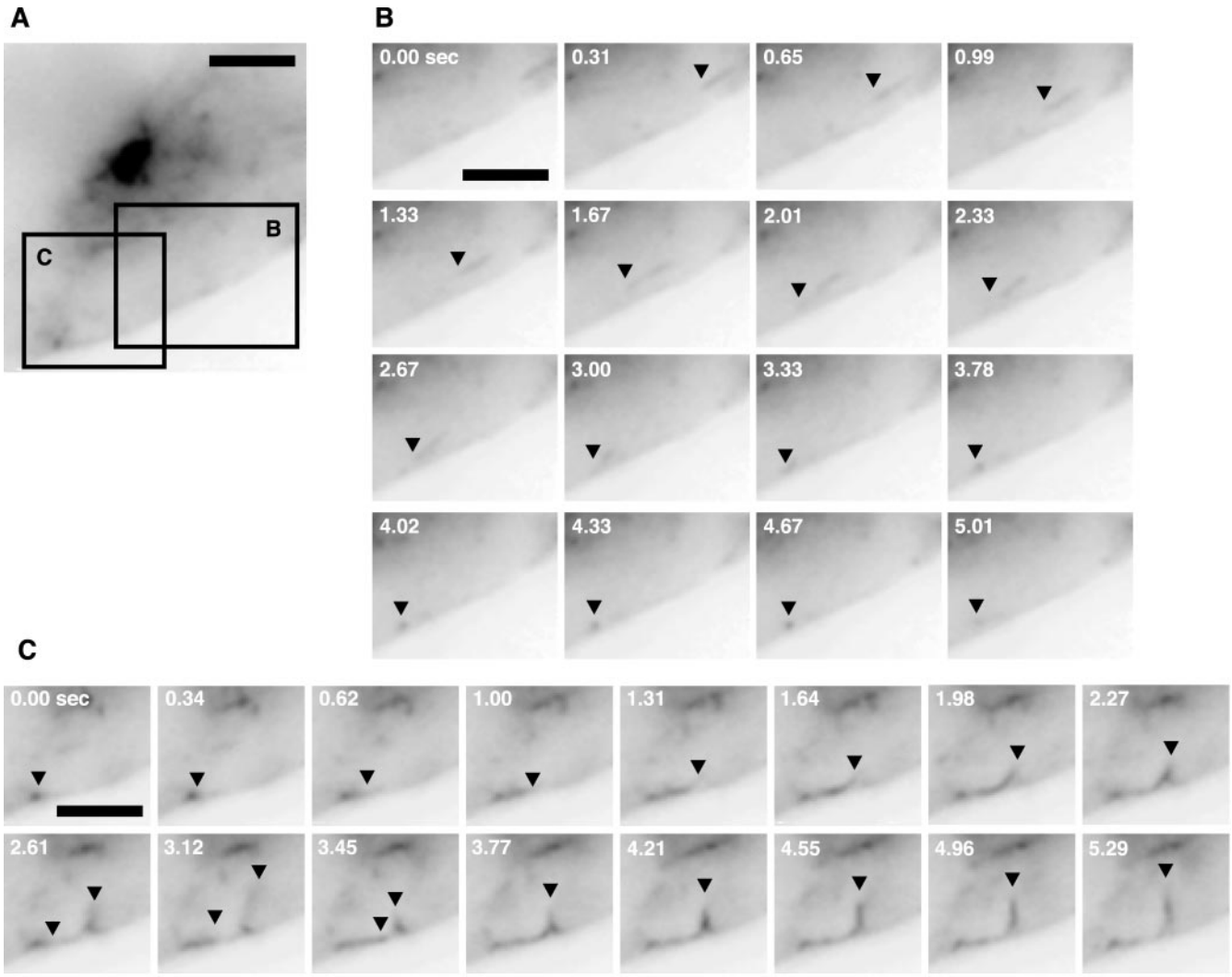

Figure 7. BSEP transport carriers also traffic toward the basolateral membrane. Also see Video 6. WIF-B9 cells infected with BSEP-YFP adenovirus were used for live cell imaging at 37°C with conventional fluorescence microscope equipped with CCD camera. (A) BSEP transport carrier distribution in WIF-B9 cell. Bar, 2 μm. Areas in A designated B and C are placed in the corresponding panels. (B) BSEP-YFP transport carriers traffic toward the basolateral membrane, denoted by black arrowhead. Times shown are relative to the first image in the series. Bar, 2 μm. (C) BSEP-YFP transport carriers traffic along the basolateral membrane which they leave and return to the region of the globular structure. BSEP-YFP transport carriers denoted by black arrowhead. Times are relative to the first image in the series. Bar, 2 μm.

10C). Furthermore, no change in the rate of fluorescence recovery after photobleaching of canalicular fluorescence was observed in these cells (Figure 10D). These results demonstrate that, in contrast to trafficking from the apical membrane to lysosomes, constitutive BSEP-YFP apical cycling is insensitive to PI 3-kinase inhibition.

In rat liver, dibytyryl cyclic AMP and taurocholate increased the amount of each ABC transporter in the canalicular membrane (Misra *et al*., 1998). Experiments were performed to determine whether dibytyryl cyclic AMP and taurocholate regulate constitutive apical cycling of BSEP in WIF-B9 cells. Dibutyryl cyclic AMP and taurocholate were added together or separately to WIF-B9 cells and fluorescence intensity of BSEP-YFP in the canalicular region was determined every 30 min for 4 h. In separate experiments, dibutyryl cyclic AMP and/or taurocholate were added to WIF-B9 cells and the canalicular region was photobleached immediately or at intervals for 3 h. Recovery of canalicular fluorescence was determined at frequent intervals for 30 min. In none of these experiments was a significant effect of cyclic AMP and/or taurocholate observed (Figure 10D; our unpublished data).

DISCUSSION

Our previous pulse-chase biochemical studies in rat liver demonstrated that BSEP traffics from Golgi through large intracellular pool(s) before selective insertion into the canalicular membrane (Kipp *et al*., 2001). The present study identifies the intracellular pools and characterizes a previously unrecognized dynamic process involving constitutive apical cycling of BSEP in a polarized hepatocyte cell line. At steady state, BSEP resides in the canalicular membrane but is also present in globular structures adjacent to the MTOC and in widely distributed tubular or vesicular transport carriers. The intracellular compartments are rab11-positive recycling endosomes. BSEP constantly and rapidly exchanges be-

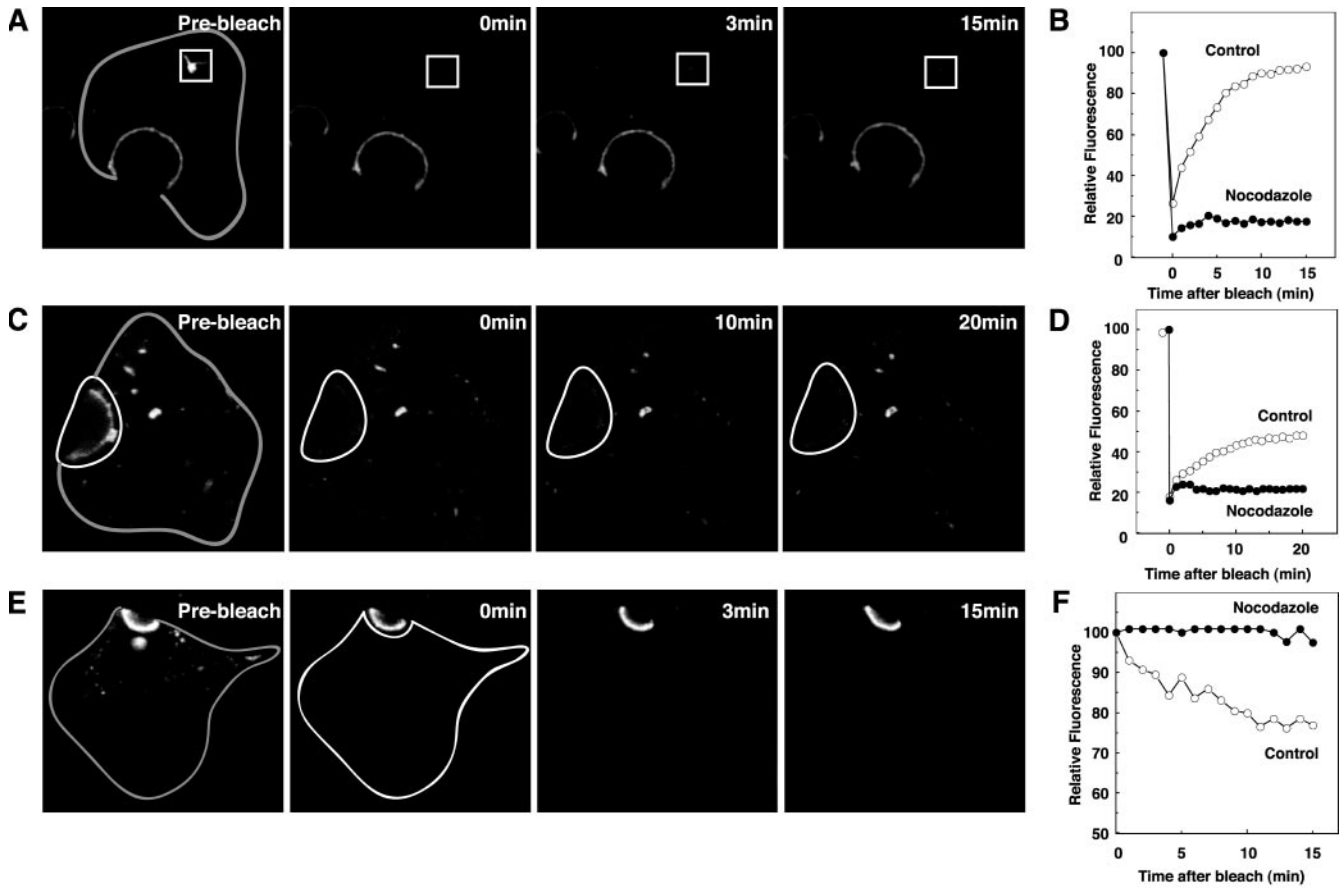

Figure 8. Requirement of microtubules for constitutive BSEP cycling. After treatment with nocodazole (33 μM) for 60 min at 37°C, WIF-B9 cells infected with BSEP-YFP adenovirus were used for live cell imaging by confocal or conventional fluorescence microscopy. (A) Microtubule disruption perturbs recovery of globular structure BSEP pool. After treatment with nocodazole for 60 min at 37°C, globular structure pool enclosed by the white line was photobleached. Time in the subsequent two panels denotes minutes postbleach. Gray line shows basolateral membrane. (B) Quantitation of BSEP-YFP recovery in globular structure pool, which was photobleached as in A. Fluorescence intensity was determined as indicated. Solid circles denote nocodazole treatment and open circles are control values. (C) Microtubule disruption perturbs recovery of the canalicular BSEP pool. After treatment with nocodazole for 60 min at 37°C, canalicular area enclosed by the white line was photobleached. Time in the subsequent two panels denotes minutes postbleach. Gray line shows basolateral membrane. (D) Quantitation of BSEP-YFP recovery in the canalicular membrane pool which was photobleached as in C. Fluorescence intensity was determined as indicated. Solid circles indicate nocodazole treatment and open circles indicate control values. (E) Microtubule disruption perturbs BSEP-YFP loss in the canalicular pool after photobleaching the entire intracellular pool. Time in the subsequent two panels denotes minutes postbleach. Gray line shows basolateral membrane. (F) Quantitation of BSEP-YFP fluorescence change in the canalicular membrane pool. The entire cell except the canalicular membrane region was photobleached as in E. Solid circles denote nocodazole treatment and open circles are control values.

tween the three sites through tubulo-vesicles carriers that move along microtubules.

Rab11, a small GTP-binding protein (Goldenring *et al*., 1996), associates with recycling endosomes in nonpolarized and polarized cells (Ullrich *et al*., 1996; Casanova *et al*., 1999). In the present study, BSEP-YFP colocalized with rab11-associated endosomes that occurred as tubulo-vesicles or globular structures proximate to the MTOC. Time-lapse imaging suggests that the globular structure functions as a recycling center that accepts endosomal carriers derived from the canalicular membrane. This process depends on intact microtubules because nocodazole inhibited BSEP trafficking between the globular structure and canalicular membranes. In addition, nocodazole reduced the association of rab11 with the BSEP-containing globular structure (our unpublished data) similar to that previously observed in MDCK cells (Casanova *et al*., 1999).

Apical plasma membrane recycling involving rab11 endosomal compartments has been described in transcytosis of pIgA in polarized MDCK cells (Ullrich *et al*., 1996; Casanova *et al*., 1999). The present study indicates that canalicular ABC transporters, which use the nontranscytotic direct route from Golgi to the apical plasma membrane (Kipp and Arias, 2000), also undergo extensive cycling associated with rab11.

In contrast to the effect of microtubule disruption, cytochalasin D and latrunculin A did not perturb trafficking of BSEP-YFP from the intracellular pools to the canalicular membrane. These characteristics of BSEP carriers resemble post-Golgi carriers, whose delivery to the plasma membrane is microtubule-dependent but not actin-dependent (Schmoranzer and Simon, 2003). However, after photobleaching all but the canalicular region, canalicular BSEP-YFP fluorescence declined by 20% in 15 min, whereas in the presence of

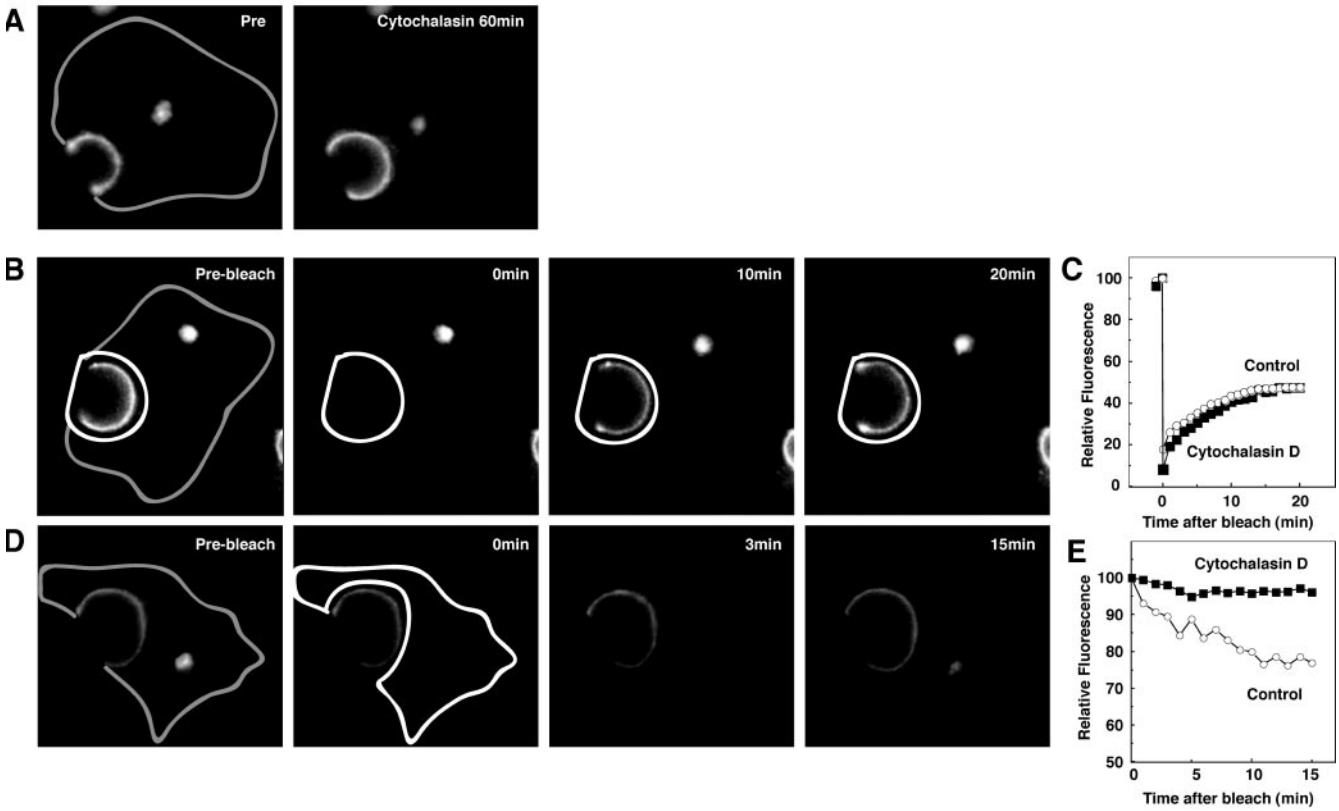

Figure 9. Requirement of actin for constitutive BSEP cycling. After treatment with cytocholasin D (1 μg/ml) for 60 min at 37°C, WIF-B9 cells infected with BSEP-YFP adenovirus were used for live cell imaging by confocal microscopy at 37°C. (A) WIF-B9 cells infected with BSEP-YFP adenovirus were imaged pre- and postcytocholasin D treatment. Cytocholasin D treatment increased the canalicular BSEP pool. Gray line shows basolateral membrane. (B) Cytocholasin D treatment does not perturb BSEP recovery in the canalicular pool. After treatment with cytocholasin D for 60 min at 37°C, the canalicular region (white line) was photobleached. Time in the second two panels denotes minutes postbleach. Gray line shows basolateral membrane. (C) Quantitation of BSEP-YFP recovery in the canalicular membrane pool. The canalicular pool was photobleached as in C. Fluorescence intensity was determined as indicated. Solid squares denote cytocholasin D treatment and open circles denote control values. (D) Cytocholasin D perturbs BSEP retrieval from the canalicular pool. After treatment with cytocholasin D for 60 min at 37°C, the entire cell except the canalicular region was photobleached. Time in the second two panels denotes minutes postbleach. Gray line shows basolateral membrane. (E) Quantitation of BSEP-YFP fluorescence change in the canalicular membrane pool. The entire cell except canalicular region was photobleached as in D. Fluorescence intensity was determined as indicated. Solid squares denote cytocholasin D treatment and open circles denote control values.

cytochalasin D or latrunculin A, canalicular fluorescence remained constant (Figure 9E). These results suggest that impaired actin polymerization inhibits cycling of BSEP-YFP from the canalicular region to intracellular sites.

Constitutive BSEP localization and apical cycling were also unaffected by PI 3-kinase inhibitors wortmannin and LY294002 (Figure 10D). In contrast, in rat liver, PI 3-kinase activity is required for increase in canalicular BSEP and other ABC transporters after taurocholate, but not dibutyryl cyclic AMP administration (Misra *et al*., 1998; Misra *et al*., 2003), and inhibition of PI 3-kinase activity stimulated apical endocytosis of several canalicular membrane proteins to lysosomes (Tuma *et al*., 2001). Constitutive apical cycling of BSEP-YFP does not include trafficking to lysosomes, which did not contain BSEP-YFP, but involves mechanisms independent of those previously shown to require active PI 3-kinase.

In contrast to results previously obtained in rat liver in vivo, taurocholate and dibutyryl cyclic AMP also had no effect in WIF-B9 cells on BSEP-YFP cycling between intracellular sites and the canalicular membrane as examined using several protocols (Figure 10D). The lack of response in the present study may be due to negligible PI 3-kinase activation in WIF-B9 cells, compared with the robust response in primary hepatocytes (Webster and Anwer, 1999; Kagawa *et al*., 2002). In addition, based on previous studies in rat liver (Gatmaitan *et al*., 1997; Misra *et al*., 1998; Kipp *et al*., 2001) in which taurocholate or dibutyryl cyclic AMP increased canalicular BSEP at 3%/min to a maximum of threefold, and the observed variability in recovery after photobleaching of BSEP-YFP in the canalicular membrane region (Figure 4B).

Whereas BSEP-YFP-containing carriers can move to the basolateral membrane, they only fuse with the canalicular membrane. This observed specificity in fusion could be due to specific motor proteins that transport BSEP-containing vesicles to their appropriate membrane domain or to downstream selectivity in membrane fusion (Burack *et al*., 2000; Setou *et al*., 2002).

In MDCK cells, myosin Vb is associated with rab11 (Lapierre *et al*., 2001) and overexpression of myosin Vb tail domain impaired transcytosis of pIgA (Lapierre *et al*., 2001). We recently observed that myosin Vb colocalizes in WIF-B9 cells with BSEP-YFP in recycling endosomes (our unpublished data). The functional significance of this association is being investigated in our laboratory.

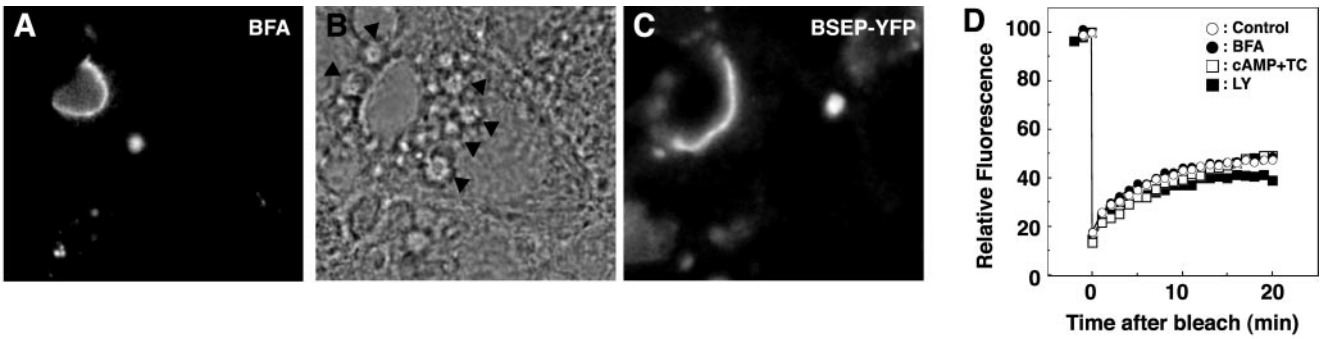

Figure 10. Mechanism of constitutive BSEP cycling in canalicular membrane. (A) After treatment with BFA (5 μg/ml) for 30 min at 37°C, WIF-B9 cells infected with BSEP-YFP adenovirus were used for live cell imaging by confocal microscopy at 37°C. B (bright field) and C (BSEP-YFP) show that LY294002 (200 μM) treatment for 60 min at 37°C produced vacuoles (closed arrowhead in B), which did not contain BSEP-YFP in C. (D) Quantitation of BSEP-YFP recovery in the canalicular membrane pool after various treatments. After treatment, canalicular BSEP-YFP pool was photobleached as in Figure 4A. Mean fluorescence intensity was determined as indicated. Open circles are control; solid circles are BFA (5 μg/ml); open squares are cyclic AMP (250 μM) + taurocholate (100 μM); solid squares are LY294002 (200 μM).

The present studies suggest that constitutive cycling of BSEP may provide a readily available mechanism to accommodate increased physiological demand for secretion of bile acids and mobilization of BSEP as well as other transporters to the canalicular membrane (Gatmaitan *et al*., 1997; Misra *et al*., 1998; Kipp *et al*., 2001). Furthermore, constitutive cycling may provide a more widely used mechanism in the regulation of membrane proteins including pumps, channels, or transporters.

ACKNOWLEDGMENTS

We thank P.J. Meier for providing cDNA; D. Jay, R. McConnell, and the Tufts/New England Medical Center imaging facility for help with several confocal microscope experiments; and Y. Sai who contributed to making BSEP-YFP adenovirus. This research was supported in part by National Institute of Diabetes and Digestive and Kidney Diseases grants DK-54785, DK-35652 (to I.M.A.) and 30-DK 34928 (Digestive Disease Center). Y.W. was the recipient of a research award from American Liver Foundation. Part of this work was presented at 53rd annual meeting of the American Association for the Study of Liver Diseases and 42nd American Society for Cell Biology annual meeting.

REFERENCES

Bartles, J.R., Feracci, H.M., Stieger, B., and Hubbard, A.L. (1987). Biogenesis of the rat hepatocyte plasma membrane in vivo: comparison of the pathways taken by apical and basolateral proteins using subcellular fractionation. J. Cell Biol. *105*, 1241–1251.

Becker, T.C., Noel, R.J., Coats, W.S., Gomez-Foix, A.M., Alam, T., Gerard, R.D., and Newgard, C.B. (1994). Use of recombinant adenovirus for metabolic engineering of mammalian cells. Methods Cell Biol. *43*, 161–189.

Bravo, P., Bender, V., and Cassio, D. (1998). Efficient in vitro vectorial transport of a fluorescent conjugated bile acid analogue by polarized hepatic hybrid WIF-B and WIF-B9 cells. Hepatology *27*, 576–583.

Burack, M.A., Silverman, M.A., and Banker, G. (2000). The role of selective transport in neuronal protein sorting. Neuron *26*, 465–472.

Casanova, J.E., Wang, X., Kumar, R., Bhartur, S.G., Navarre, J., Woodrum, J.E., Altschuler, Y., Ray, G.S., and Goldenring, J.R. (1999). Association of Rab25 and Rab11a with the apical recycling system of polarized Madin-Darby canine kidney cells. Mol. Biol. Cell *10*, 47–61.

Chardin, P., and McCormick, F. (1999). Brefeldin A: the advantage of being uncompetitive. Cell *97*, 153–155.

Decaens, C., Rodriguez, P., Bouchaud, C., and Cassio, D. (1996). Establishment of hepatic cell polarity in the rat hepatoma-human fibroblast hybrid WIF-B9. A biphasic phenomenon going from a simple epithelial polarized phenotype to an hepatic polarized one. J. Cell Sci. *109*, 1623–1635.

Durrbach, A., Raposo, G., Tenza, D., Louvard, D., and Coudrier, E. (2000). Truncated brush border myosin I affects membrane traffic in polarized epithelial cells. Traffic *1*, 411–424.

Gatmaitan, Z.C., Nies, A.T., and Arias, I.M. (1997). Regulation and translocation of ATP-dependent apical membrane proteins in rat liver. Am. J. Physiol. *272*, G1041–G1049.

Gerloff, T., Stieger, B., Hagenbuch, B., Madon, J., Landmann, L., Roth, J., Hofmann, A.F., and Meier, P.J. (1998). The sister of P-glycoprotein represents the canalicular bile salt export pump of mammalian liver. J. Biol. Chem. *273*, 10046–10050.

Goldenring, J. R., Smith, J., Vaughan, H. D., Cameron, P., Hawkins, W., and J., N. (1996). Rab11 is an apically located small GTP-binding protein in epithelial tissues. Am. J. Physiol. *270*, G515–G525.

Gottlieb, T.A., Ivanov, I.E., Adesnik, M., and Sabatini, D.D. (1993). Actin microfilaments play a critical role in endocytosis at the apical but not the basolateral surface of polarized epithelial cells. J. Cell Biol. *120*, 695–710.

He, T.C., Zhou, S., da Costa, L.T., Yu, J., Kinzler, K.W., and Vogelstein, B. (1998). A simplified system for generating recombinant adenoviruses. Proc. Natl. Acad. Sci. USA *95*, 2509–2514.

Hunziker, W., Whitney, J.A., and Mellman, I. (1991). Selective inhibition of transcytosis by brefeldin A in MDCK cells. Cell *67*, 617–627.

Ihrke, G., Neufeld, E.B., Meads, T., Shanks, M.R., Cassio, D., Laurent, M., Schroer, T.A., Pagano, R.E., and Hubbard, A.L. (1993). WIF-B cells: an in vitro model for studies of hepatocyte polarity. J. Cell Biol. *123*, 1761–1775.

Kagawa, T., Varticovski, L., Sai, Y., and Arias, I.M. (2002). Mechanism by which cAMP activates PI3-kinase and increases bile acid secretion in WIF-B9 cells. Am. J. Physiol. *283*, C1655–C1666.

Kipp, H., and Arias, I.M. (2000). Newly synthesized canalicular ABC transporters are directly targeted from the Golgi to the hepatocyte apical domain in rat liver. J. Biol. Chem. *275*, 15917–15925.

Kipp, H., Pichetshote, N., and Arias, I.M. (2001). Transporters on demand: intrahepatic pools of canalicular ATP binding cassette transporters in rat liver. J. Biol. Chem. *276*, 7218–7224.

Lapierre, L.A., Kumar, R., Hales, C.M., Navarre, J., Bhartur, S.G., Burnette, J.O., Provance, D.W.J., Mercer, J.A., Bahler, M., and Goldenring, J.R. (2001). Myosin vb is associated with plasma membrane recycling systems. Mol. Biol. Cell *12*, 1843–1857.

Lin, S.H., Culic, O., Flanagan, D., and Hixson, D.C. (1991). Immunochemical characterization of two isoforms of rat liver ecto-ATPase that show an immunological and structural identity with a glycoprotein cell-adhesion molecule with Mr 105,000. Biochem. J. *278*, 155–161.

Misra, S., Ujhazy, P., Gatmaitan, Z., Varticovski, L., and Arias, I.M. (1998). The role of phosphoinositide 3-kinase in taurocholate-induced trafficking of ATP-dependent canalicular transporters in rat liver. J. Biol. Chem. *273*, 26638–26644.

Misra, S., Varticovski, L., and Arias, I.M. (2003). Mechanisms by which cAMP increases bile acid secretion in rat liver and canalicular membrane vesicles. Am. J. Physiol. *285*, 316–324.

Newman, T.M., Tian, M., and Gomperts, B.D. (1996). Ultrastructural characterization of tannic acid-arrested degranulation of permeabilized guinea pig eosinophils stimulated with GTP-gamma-S. Eur J. Cell Biol. *70*, 209–220.

Nies, A.T., Cantz, T., Brom, M., Leier, I., and Keppler, D. (1998). Expression of the apical conjugate export pump, Mrp2, in the polarized hepatoma cell line, WIF-B. Hepatology *28*, 1332–1340.

Paschal, B.M., Holzbaur, E.L., Pfister, K.K., Clark, S., Meyer, D.I., and Vallee, R.B. (1993). Characterization of a 50-kDa polypeptide in cytoplasmic dynein preparations reveals a complex with p150GLUED and a novel actin. J. Biol. Chem. *268*, 15318–15323.

Polishchuk, R.S., Pentima, A.D., and Lippincott-Schwartz, J. (2004). Delivery of raft-associated, GPI-anchored proteins to the apical surface of polarized MDCK cells by a transcytotic pathway. Nat. Cell Biol. *6*, 297–307.

Prydz, K., Hansen, S.H., Sandvig, K., and van Deurs, B. (1992). Effects of brefeldin A on endocytosis, transcytosis and transport to the Golgi complex in polarized MDCK cells. J. Cell Biol. *119*, 259–272.

Rosin-Arbesfeld, R., Ihrke, G., and Bienz, M. (2001). Actin-dependent membrane association of the APC tumour suppressor in polarized mammalian epithelial cells. EMBO J. *20*, 5929–5939.

Sai, Y., Nies, A.T., and Arias, I.M. (1999). Bile acid secretion and direct targeting of mdr1-green fluorescent protein from Golgi to the canalicular membrane in polarized WIF-B cells. J. Cell Sci. *112*, 4535–4545.

Schell, M.J., Maurice, M., Stieger, B., and Hubbard, A.L. (1992). 5′nucleotidase is sorted to the apical domain of hepatocytes via an indirect route. J. Cell Biol. *119*, 1173–1182.

Schmitt, M., Kubitz, R., Lizun, S., Wettstein, M., and Haussinger, D. (2001). Regulation of the dynamic localization of the rat Bsep gene-encoded bile salt export pump by anisoosmolarity. Hepatology *33*, 509–518.

Schmoranzer, J., and Simon, S.M. (2003). Role of microtubules in fusion of post-Golgi vesicles to the plasma membrane. Mol. Biol. Cell *14*, 1558–1569.

Setou, M., Seog, D.H., Tanaka, Y., Kanai, Y., Takei, Y., Kawagishi, M., and Hirokawa, N. (2002). Glutamate-receptor-interacting protein GRIP1 directly steers kinesin to dendrites. Nature *417*, 83–87.

Slimane, T.A., Trugnan, G., Van IJzendoorn, S.C., and Hoekstra, D. (2003). Raft-mediated trafficking of apical resident proteins occurs in both direct and transcytotic pathways in polarized hepatic cells: role of distinct lipid microdomains. Mol. Biol. Cell *14*, 611–624.

Strautnieks, S.S., *et al*. (1998). A gene encoding a liver-specific ABC transporter is mutated in progressive familial intrahepatic cholestasis. Nat. Genet. *20*, 233–238.

Tuma, P.L., Finnegan, C.M., Yi, J.H., and Hubbard, A.L. (1999). Evidence for apical endocytosis in polarized hepatic cells: phosphoinositide 3-kinase inhibitors lead to the lysosomal accumulation of resident apical plasma membrane proteins. J. Cell Biol. *145*, 1089–1102.

Tuma, P.L., Nyasae, L.K., Backer, J.M., and Hubbard, A.L. (2001). Vps34p differentially regulates endocytosis from the apical and basolateral domains in polarized hepatic cells. J. Cell Biol. *154*, 1197–1208.

Ullrich, O., Reinsch, S., Urbe, S., Zerial, M., and Parton, R.G. (1996). Rab11 regulates recycling through the pericentriolar recycling endosome. J. Cell Biol. *135*, 913–924.

Webster, C.R., and Anwer, M.S. (1999). Role of the PI3K/PKB signaling pathway in cAMP-mediated translocation of rat liver Ntcp. Am. J. Physiol. *277*, G1165–G1172.